NJC

New Journal of Chemistry

A journal for new directions in chemistry

Accepted Manuscript

This article can be cited before page numbers have been issued, to do this please use: R. Varshney, S. Kumar, K. Ghosh and D. Patra, *New J. Chem.*, 2020, DOI: 10.1039/C9NJ05322K.

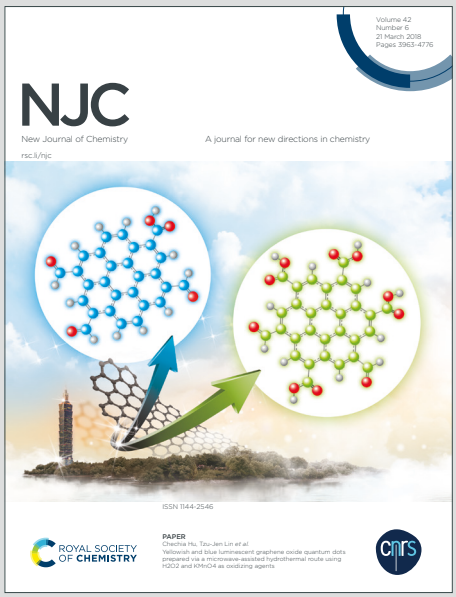

This is an Accepted Manuscript, which has been through the Royal Society of Chemistry peer review process and has been accepted for publication.

Accepted Manuscripts are published online shortly after acceptance, before technical editing, formatting and proof reading. Using this free service, authors can make their results available to the community, in citable form, before we publish the edited article. We will replace this Accepted Manuscript with the edited and formatted Advance Article as soon as it is available.

You can find more information about Accepted Manuscripts in the Information for Authors.

Please note that technical editing may introduce minor changes to the text and/or graphics, which may alter content. The journal's standard Terms & Conditions and the Ethical guidelines still apply. In no event shall the Royal Society of Chemistry be held responsible for any errors or omissions in this Accepted Manuscript or any consequences arising from the use of any information it contains.

View Article Online
DOI: 10.1039/C9NJ05322K

ARTICLE

Fabrication of Dual Catalytic Microcapsules by Mesoporous Graphitic Carbon Nitride (mpg-C_3N_4) Nanoparticles-Enzyme Conjugates Stabilized Emulsions.

Received 00th January 20xx,
Accepted 00th January 20xx

DOI: 10.1039/x0xx00000x

Rohit Varshney[a], Sushil Kumar[b], Kaushik Ghosh[b] and Debabrata Patra[a*]*

Emulsion templated microcapsules (MCs) were fabricated by simultaneous self-assembly and crosslinking of mpg-C_3N_4 nanoparticles (NPs) and lipase conjugates at oil-water interface. The presence of both enzymes and mpg-C_3N_4 NPs at the interface make the MCs an ideal candidate for dual catalysis i.e. biocatalysis as well as photocatalysis. The biocatalytic activity of the MCs is found to be 1.2 fold higher compare to free enzymes and the visible light induced dye degradation rate by mpg-C_3N_4 immobilized MCs is 1.7 times higher than NPs only. Most importantly, these MCs are capable of performing biocatalytic and photocatalytic activity simultaneously in mixture of substrates.

Introduction

Intensive industrial and agricultural activities have led to a considerable contamination of soil and water by toxic pollutants, which may have catastrophic impact on human health and environment.[1, 2] Emerging pollutants like pharmaceutical waste, flame retardants, dyes and pesticides are of great concern and there is a global need for the development of new, low-cost and eco-friendly treatments.[3, 4] Most prior attempts focus on photodegradation and biodegradation to address the waste remediation.[5, 6] In photocatalytic degradation, photocatalysts absorb light and produce electron/hole pairs. The photogenerated hole produces reactive radicals and degrades the contaminants. Aromatic hydrocarbons and chlorinated aromatic hydrocarbons, phenols, pesticides dyes can be decontaminated by this process.[7-9] Biological degradation refers to the elimination of pollutants either by enzymatic oxidation or by relying on the metabolic activity of living microorganism like bacteria and fungi.[10] Due to low cost and energy requirements, biological treatments have been widely accepted to treat waste water containing azo dyes. However, separate degradation of waste materials increases cost, thus the problem of sequential treatments can be overcome if both the degradations can occur together.[11] An emerging approach combines both photodegradation and biodegradation to minimize the processing steps and often times the combined approach leads to complete mineralization of the pollutants.[12-15] This strategy requires co-immobilization of the catalysts on the carriers and catalytic cycle of one catalyst should not get hindered by the presence of another catalyst.

Co-immobilization of catalysts requires a robust carrier with high surface area and also it needs an easy fabrication procedure for large scale productions. In this context, Pickering emulsions stabilized by colloidal particles can play an important role due to their enhanced stability, environmental friendliness as well as low fabrication cost.[16, 17] Apart from their usage in encapsulation and drug delivery, the colloidal microcapsules (MCs) were also successfully applied in catalysis. In a typical emulsion catalysis, the catalysts are located either inside or outside of the emulsion droplets. For example, nanoparticles (NPs) stabilized oil-in-water (o/w) emulsions act as a microreactor for solubilizing hydrophobic catalysts and provide a template for biphasic reaction.[18, 19] Similarly water-in-oil (w/o) type Pickering emulsions produces aqueous microenvironment to protect hydrophilic components from the organic media.[20-22] These types of emulsions can be used in various biocatalytic systems, confining enzymes in organic media.[23, 24] In other approach emulsion droplets act as scaffold for immobilization of catalysts at oil-water interface. Both synthetic and biocatalysts have been immobilized at the interface to perform desired catalysis.[25, 26] Similar approach can be adopted to construct MCs which will be able to perform both photocatalysis and biocatalysis simultaneously.

Herein, we report a simple approach for the fabrication of stable dual catalytic MCs by simultaneous self-assembly and crosslinking of mpg-C_3N_4 nanoparticle and enzyme conjugates at oil-water interface. The presence of both lipase and mpg-C_3N_4 NPs at the interface make the MCs an ideal candidate for dual catalysis i.e. biocatalysis as well as photocatalysis. To best of our knowledge this is the first example of catalytic MCs derived from emulsion droplet exhibiting dual catalytic activity in respective substrates. Most importantly, these MCs are capable of performing biocatalytic and photocatalytic activity simultaneously in mixture of substrates.

[a] *Institute of Nano Science and Technology, Habitat Centre, Phase-10, Sector-64, Mohali, Punjab, 160062, India.*
[b] *Institute of Nano Science and Technology, Habitat Centre, Phase-10, Sector-64, Mohali, Punjab, 160062, India.*
† Footnotes relating to the title and/or authors should appear here.
Electronic Supplementary Information (ESI) available: [details of any supplementary information available should be included here]. See DOI: 10.1039/x0xx00000x

View Article Online
DOI: 10.1039/C9NJ05322K

Experimental Section

Materials

Dicyandiamide 99%, Amano Lipase PS from *Burkholderia cepacia*, 1,2,4-Trichlorobenzene(≥99%), Nile red, Bradford Reagent, Bovine Serum Albumin (analytical standard), Rhodamine B, p-Nitrophenyl palmitate were purchased from Sigma-Aldrich and used as received without further modification. Cetyl trimethyl ammonium bromide (CTAB), and Tetraethyl orthosilicate was purchased from TCI. Glycine, Gum Arabic, TritonX-100, Calcium chloride, 2-Propanol were purchased from HIMEDIA. All other solvents were of analytical reagent grade. Millipore water (18.2 MΩ•cm at 25 °C) was used in all experiments.

Preparation of mesoporous graphitic Carbon Nitride nanoparticles (mpg-C_3N_4):

Synthesis of mesoporous MCM41: Synthesis of MCM41 was followed as per literature reported protocol with little modification.[27] In a typical procedure, 1.5 g of CTAB was added to 120 mL of distilled water and then was heated to 80 °C. To this solution, 1.75 mL of 2.0 M of NaOH was added. After 5 minutes of stirring, 2.36 g of Tetraethyl orthosilicate (TEOS) was added rapidly and was allowed to stir at 80 °C for 2 hours. White precipitation was observed and was collected via centrifugation at 3000 rpm. Finally, the precipitate was dried at 60 °C to get solid powder. To remove the surfactant from the powder, the white precipitate was heated at 550 °C to get the MCM41 template.

Synthesis of mesoporous graphitic carbon nitride (mpg- C_3N_4):

0.5 g of the MCM41 template was taken in a beaker and 4M of dicyandiamide (DCDA) (3 mL) was added under slow stirring at 45 °C till the slurry became dry. The solid content was collected and then heated at 550 °C for 5 hours to get the g-C_3N_4 impregnated MCM41 template. The solid was then added to 10 mL of 10% HF solution and kept it for 5 hours in a fume hood for the complete removal of MCM-41 template. The solution was then centrifuged at 5000 rpm for 15 minutes to get yellow colored precipitation. The precipitation was redispersed in 10 mL of water and again was collected by centrifugation at 5000 rpm for 15 min. This process was repeated five times for complete removal of HF from the solution. Finally, the precipitate was dried at 60°C overnight to get yellow coloured mesoporous g-C_3N_4 structure.

Preparation of Microcapsules (MCs):

The formation of MCs is based on supramolecular assembly of lipase and NP in aqueous solution. The fabrication of MCs is a two-step process. First step involves the formation of neutral or low valent charge conjugates by mixing 470µL of NPs (1mg/mL in 10mM glycine-HCl buffer; pH 3.0±0.5 adjusted with 1M HCl) with 330µL of Amano Lipase PS (1mg/mL in 10mM glycine-NaOH buffer; pH 7.4±0.5 adjusted with 1M NaOH). In second step, 50µL of 1,2,4-Trichlorobenzene was subsequently added to a nanoparticle-enzyme conjugate solution (800µL) followed by vigorous mechanical agitation for 30s. In this process a spontaneous self-assembly and extended cross-linking of nanoconjugates occurred and it resulted in formation of stable MCs. These MCs were washed three times to remove excess nanoconjugates prior to any characterization.

Enzyme activity assay:

The enzymatic activity of the MCs was determined spectrophotometrically by using an assay based on hydrolysis of p-Nitrophenyl palmitate (p-NPP). Solution A: 3 mg/mL of p-NPP in 2-propanol; Solution B: 110 mg of gum arabic and 400 µL of Triton X-100 was dissolved in 100 mL of Tris buffer (50 mM, pH 7.4). Solution C: 166.5 mg of calcium chloride in 100 mL of deionised water (DI) water. 45 µL of solution A and 405 µL of solution B were added to 250 µL of calcium chloride solution. The final volume was adjusted to 1.5 mL by adding Tris buffer (50 mM). The mixture was incubated for 10 minutes at 60 °C. 50 µL of MCs were added immediately to the substrate solution. Hydrolysis of the substrate to p-Nitrophenol was monitored by measuring the absorbance at 410 nm up to 10 minutes at an interval of 60 seconds. The assays were implemented in duplicate and triplicates, and averages were reported.

Photodegradation study:

The photocatalytic performance of MCs was investigated by RhB degradation study. Pyrex photocatalytic reaction apparatus with 400 W Xe arc lamp (with a filter λ > 400 nm) was used as a light source. The apparatus was kept at a constant temperature through integrated circulating water system. The freshly prepared MCs were added to the 8 mL aqueous solution of RhB (12µM). Prior to light irradiation, the suspension was stirred for 20 min to reach adsorption-desorption equilibrium. The solution was gently stirred throughout the experiment to prevent the damage of MCs. During the course of the reaction, 500 µL aliquot of reaction mixture was collected for UV-Vis analysis at 20 mins intervals up to 140 mins. In a control experiment, NPs suspension (1mg/mL) was added to same volume of RhB aqueous solution. The degradation efficiency of organic dye RhB was analysed by an UV-Vis spectrophotometer at wavelength 554 nm. All photocatalytic experiments were carried out at 25 °C.

Characterization

All the preliminary characterization of MCs was carried out by optical microscopy (Olympus BX53F microscope). MCs were transferred to a glass slide with the aqueous solution for imaging. Fluorescent samples and dried samples were also characterized by the same optical microscope. The Zeta potential analysis was carried out by Zetasizer Nano ZSP (ZEN5600) instrument. The phase purity and crystalline nature of the graphitic carbon nitride nanostructures were determined by Bruker powder X-ray diffractometer (PXRD, D8 ADVANCE with DAVINCI design) operated at 40 KeV and 25 mA with Cu Kα radiation in the range of 10–800 with a step of 0.028. The surface area and pore size analysis of the samples were determined by nitrogen physisorption at 77K in Autosorb IQ Quantachrome instrument using the BET and the Barrett-Joyner-Halenda equation. Transmission electron microscopy (TEM) was carried out with a JEOL JEM-2100 microscope operating at acceleration voltage 200KV. Confocal laser scanning microscopy

View Article Online
DOI: 10.1039/C9NJ05723K

(CLSM) was carried out with Carl Zeiss microscopy LSM 880. The Photocatalytic activity was further evaluated by the degradation of model Rhodamine B (RhB) dye spectrophotometrically monitored by optical absorption values (at 554 nm on UV-2600 ultraviolet-visible spectrophotometer SHIMADZU) during the photodegradation process. The biocatalytic assay was evaluated by hydrolysis of para-Nitrophenyl palmitate into p-Nitrophenol (yellow coloured solution) and palmitic acid and the concentration of p-Nitrophenol formed was spectrophotometrically monitored by optical absorption values at 410nm. UV-vis diffuse reflectance spectroscopy (UV-vis DRS) was recorded on a Agilent Technologies Cary Series UV-Vis spectrophotometer in the range 200-800 nm at room temperature, with a $BaSO_4$ standard used as the reference. The Mott-Schottky plot was obtained at a frequency of 0.1 kHz in an aqueous solution of 1.0M KOH by Metrohm Autolab (MULTI AUTOLAB M204).

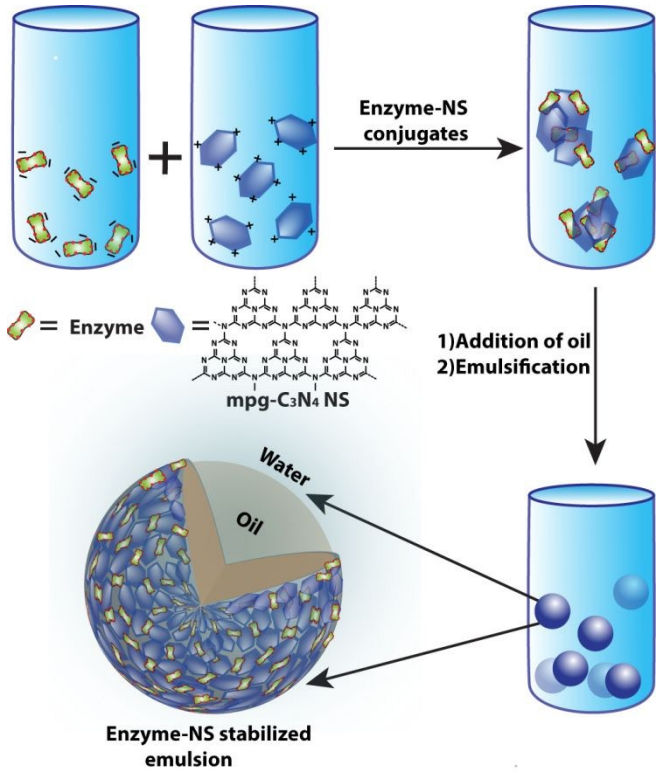

Figure 1. Schematic representation for fabrication of dual catalytic MCs stabilized by mpg-C_3N_4 nanoparticle-enzyme conjugates at oil-water interface.

Results and Discussions

The dual catalytic MCs presented here are consisted of mesoporous graphitic carbon nitride (mpg-C_3N_4) NPs and enzymes. The NPs used in this study was synthesized as per the previous literature report which has been mentioned in the experimental section and the average crystallite size of NP was 4.9 nm (See SI Fig. S1-S4). The freshly prepared aqueous dispersion of NPs showed a pH dependent zeta potential behaviour due to the presence of terminal amine group.[28] In this study the zeta potential of NPs in 10 mM glycine-HCl buffer (pH 3.5±0.5) was +19.1 ± 0.26 mV. The lipase from Burkholderia cepacia (pI = 5.2) was used as enzyme component to bind with positively charged NPs. The enzyme was dispersed in 10 mM glycine-NaOH solution (pH 7.4±0.5) and the zeta potential of the enzyme was -10.5 ± 4.7 mV. In order to stabilize the emulsion, the formation of neutral charge conjugates was crucial and the charge of the NP-enzyme complex was assessed by zeta potential titration. The conjugates were formed by mixing NPs and enzymes at a fixed concentration (See SI Fig. S5) and the effective charge of the complex was recorded to -0.556 ± 0.16 mV. Next step involves the addition of oil (chloroform) to the complex solution followed by vigorous mechanical agitation which resulted in formation of spherical MCs (Figure 1). The entrapment of NP-enzyme conjugates at oil-water interface as well as their extended crosslinking at the interface stabilized the MCs.

The freshly prepared MCs were analyzed by Optical Microscope (OM) and the OM micrograph revealed the size of MCs ranging from 20 µm to 150 µm (Figure 2a). The slow evaporation of organic solvent from the inner core of the MCs resulted crumbled morphology (Figure 2a inset) however the shape integrity was maintained inferring the stability of the MCs. To determine the emulsions type, Nile red was used as an oil soluble dye. Successful encapsulation of dye inside the MCs was examined by fluorescence microscope and red fluorescent image of MCs (Figure 2b) confirmed the formation of oil-in-water emulsion in this approach. Blue emission, an inherent property of mpg-C_3N_4 was observed when MCs were excited by UV light under fluorescence microscope (Figure 2c). Further investigation of the MCs by confocal laser scanning microscopy (CLSM) showed that the blue emission was observed only from the surface of the MCs under 405 nm excitation (Figure 2d). The Z-stacking image (Figure 2d inset) of MC also confirmed the presence of NP selectively at the surface of capsules. The immobilization of enzyme on the surface of MCs was confirmed in earlier report.[29]

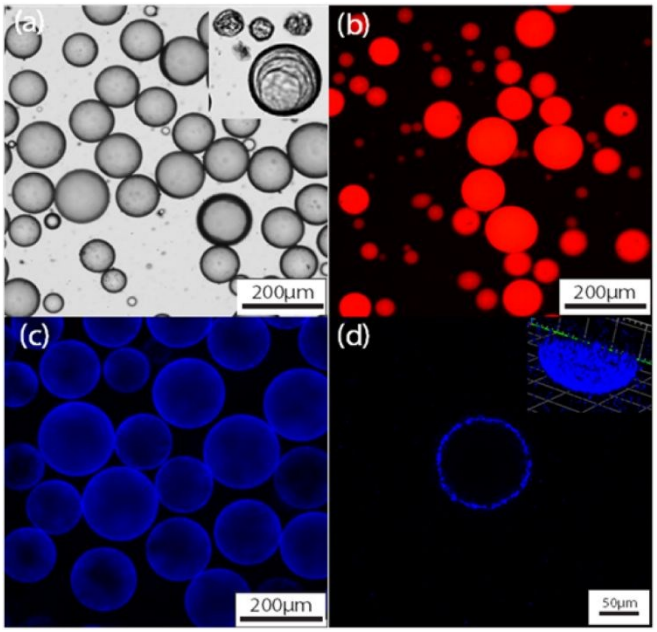

Figure 2. (a) Optical micrograph images of mpg-C_3N_4-enzyme immobilized MCs, inset shows dried MCs with wrinkle formation (b) Fluorescent microscopy image of Nile red encapsulated MCs. (c) Fluorescence microscope image of MCs (d) Confocal microscopy image of microcapsule, inset micrograph shows confocal z-stack 3D reconstuct image of MC.

View Article Online
DOI: 10.1039/C9NJ05322K

The presence of NP-enzyme conjugates at the surface of MCs provides the substrate accessibility for the dual catalysis. To assess the biocatalytic activity of the MCs, it is important to quantify the amount of enzyme immobilized on MCs. The yield of lipase immobilization onto the MCs was estimated by measuring the amount of residual enzyme in the buffer system using Bradford protein assay.[30] The measurement showed that ~ 30% of the enzyme remained in the supernatant phase of MCs, indicating that 70% of the enzyme was successfully immobilized on the MCs. The enzymatic activity of the MCs was determined spectrophotometrically by using an assay based on hydrolysis of p-Nitrophenyl palmitate (p-NPP) (Figure 3a).[31] The catalytic activity for microcapsules was found to be 1.2 fold higher compare to free enzyme (Inset; Figure 3a) with no detectable autohydrolysis of substrate observed. The higher activity of immobilized lipase arises due to the presence of hydrophobic (oil) environment in the system.[32]

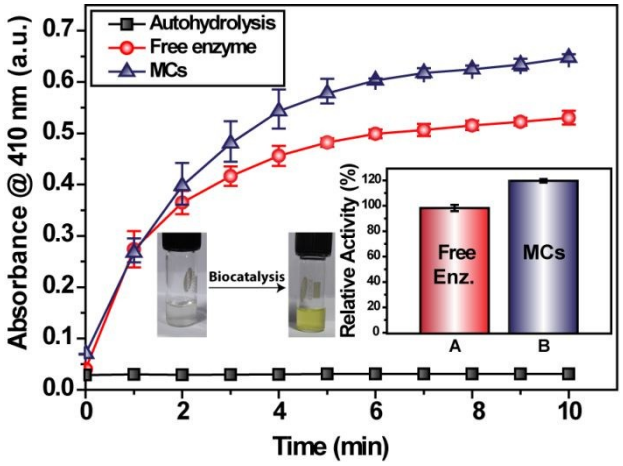

Figure 3. Activity assays of MCs and free lipase in Tris Buffer (50 mM) and inset shows the relative activity (free lipase solution = 100%).

The photocatalytic activity of the MCs has been examined by the degradation of Rhodamine B (RhB) dye under visible light irradiation and the process was monitored by measuring the absorbance of dye at 554 nm. Prior to photo irradiation, the adsorption equilibrium state was reached in 20 minutes for all materials tested in dark. After the adsorption equilibrium, the reaction mixture was irradiated with visible light to perform the dye degradation process. MCs degraded the dye completely in 140 minutes as shown in Figure 4a whereas only 94 % degradation was observed in presence of mpg-C_3N_4 colloidal suspension (See SI Fig. S6). The corresponding first-order kinetics plot in Fig 4b explained that the MCs exhibits the faster degradation rate (k_{MCs} = 0.026 min^{-1}; $K_{mpg\text{-}CN}$ = 0.0130 min^{-1}), which is almost 1.73 times higher than that of colloidal suspension of mpg-C_3N_4. The faster kinetics could be the result of better visible light utilization by mpg-C_3N_4 nanoparticles upon immobilization on emulsion surface. The electron gripping effect by amide bond, abundant in proteins, might supress the recombination probability of electron-hole pair, thus enhance the photocatalytic activity of mpg-C_3N_4-enzyme conjugated MCs.[33] Further the dye degradation mechanism was investigated by tracking several active species such as ·OH, $·O^{2-}$, electrons (e-) and holes (h^+) produced during photolysis (Fig 4c). The degradation efficiency (D) can be calculated as D= (C_0-C/C_0) x100, where C_0 and C are the equilibrium concentration of the dye before and after light irradiation, respectively. As shown in Figure 4c, the degradation of RhB was significantly (< 5%) inhibited by addition of 10% (v/v) TEOA (Triethanolamine; hole scavenger) whereas in presence of DMSO (Dimethyl sulfoxide; electron trapper) 75 % dye degradation still occurred. It clearly implies that the photogenerated holes were the key factor for decolouration of RhB.

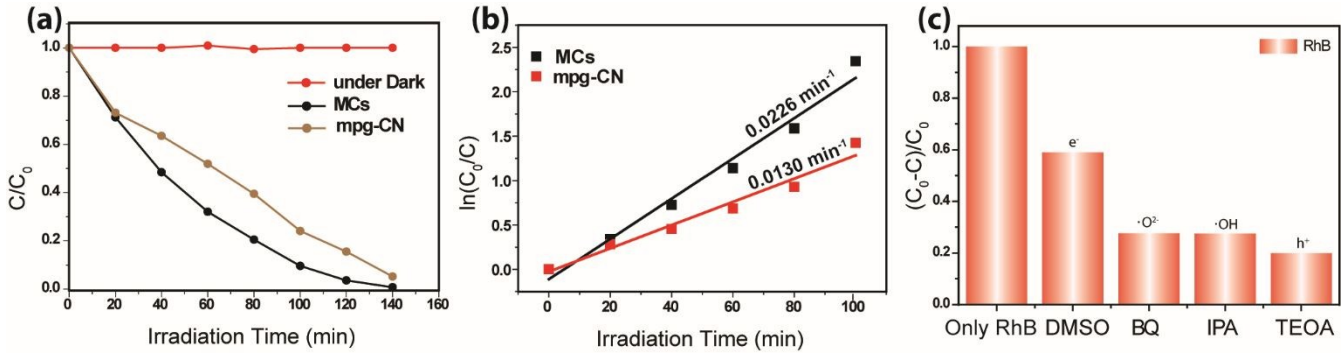

Figure 4. (a) Photodegradation study of RhB in presence of MCs, aqueous solution of mpg-C_3N_4 and absence of visible light. (b) The corresponding first-order kinetics plots of mpg-C_3N_4 and MCs. (c) Photocatalytic degradation efficiency of mpg-C_3N_4/enzyme immobilized MCs in presence of various scavengers.

To probe the generation of reactive oxygen intermediates during the photolysis process, isopropyl alcohol (IPA; hydroxyl radical scavenger) and benzoquinone (2mM) (BQ; superoxide radical scavenger) were added to reaction mixture. The degradation was supressed in presence of BQ and the results indicate that a large number of $\cdot O^{2-}$ were generated when mpg-C_3N_4 irradiated under visible light. Degradation of the dyes was supressed to 25 % when IPA was added to the solution concluding that ·OH radical was produced through the reaction of $\cdot O^{2-}$ with H+ during the course of reaction.

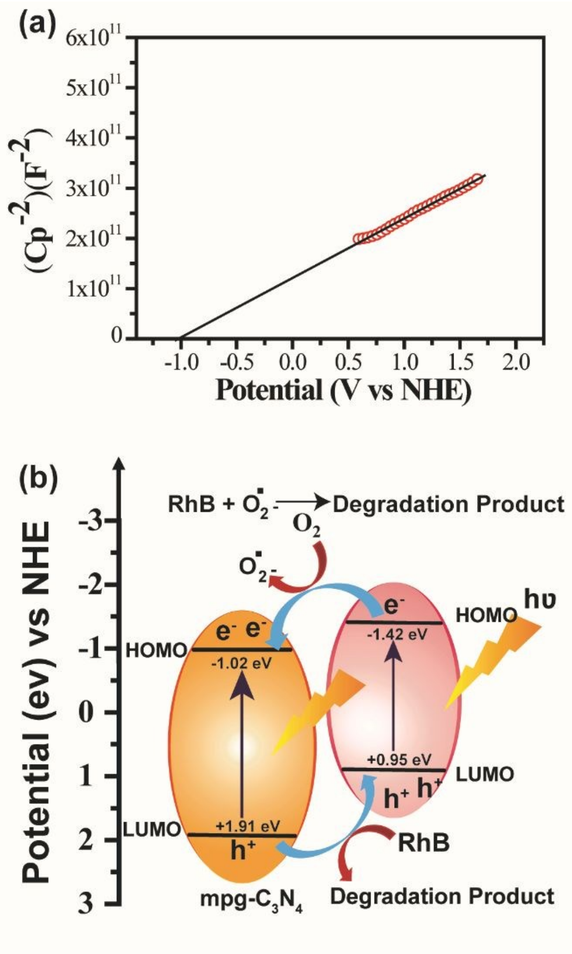

Figure 5. (a) Mott-Schottky (MS) plot of the mpg-C_3N_4 electrodes. (b) Schematic diagram showing the process of the photocatalytic degradation of RhB over the mpg-C_3N_4 nanoparticle.

The scavenger studies infer that RhB dyes have been degraded via two pathways (a) direct photocatalytic process and (b) dye sensitization process. In direct photocatalytic process, incident photon on semiconductor catalysts generates hole in the valance band (VB) and electron in the conduction band (CB). These photogenerated species either directly react with dye or produce reactive radicals for the degradation of dye molecules. In dye photosensitization process, the photo excited dyes adsorbed on the semiconductor surface can transfer their electrons into the CB of the semiconductors and readily react with O_2 to form $\bullet O_2^-$ radicals for the degradation of dyes. To investigate further, conduction band potential (E_{CB}) and valence band potential (E_{VB}) of mpg-C_3N_4 NPs were estimated by diffuse reflectance spectroscopy analysis (DRS; See SI Figure S7) and Mott-Schottky plot (Figure 5a). The minima E_{CB} and E_{VB} are estimated to be -1.02 eV and 1.91 eV for mpg-C_3N_4 NPs respectively. As per literature report, the highest occupied molecular orbital (HOMO) and the lowest unoccupied molecular orbital (LUMO) levels of RhB are about 0.95 eV and −1.42 eV, respectively.[34] From the energy level diagram as depicted in Figure 5b, it is evident that photogenerated holes (h^+) are transferred to the highest occupied molecular orbital (HOMO) of RhB and thus influence the RhB degradation to CO_2, H_2O and other products via direct photocatalytic process. On other hand, in photosensitization process, photo excited RhB dyes transfer the electron from LUMO to low lying CB of mpg-C_3N_4 NPs where it reacts further with O_2 molecules on the photocatalyst to generate •OH and $\bullet O_2^-$ radicals for dye degradation process.

The key challenge of a multiple catalysts loaded system is their ability to catalyze the reactions in mixture of substrates. In this experiment, the mpg-C_3N_4 NP-enzyme conjugates composed MCs were added to mixture of p-NPP (substrate for enzyme) and RhB (substrate for mpg-C_3N_4). Figure 6 compares the catalytic activity of MCs in individual substrate versus in a mixture of substrates. It is important to mention that the catalytic activity in individual substrate was assumed to be 100 % for better comparison. The biocatalytic activity of the MCs was calculated to 75% whereas the photocatalytic activity was estimated to 84% in the reaction mixture. These results clearly demonstrated that MCs are able to perform dual catalytic activity simultaneously in a mixture of substrates.

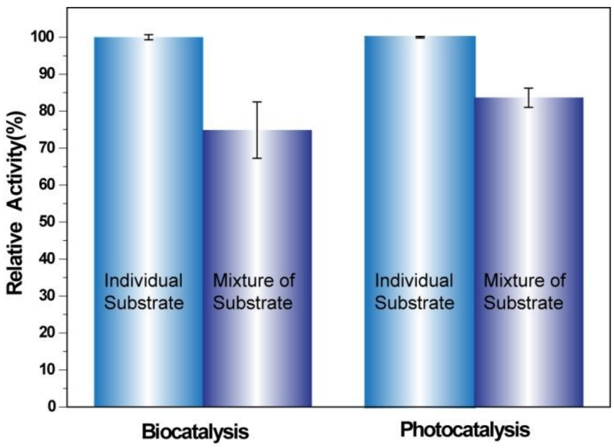

Figure 6. Assessment of biocatalytic activity and photocatalytic activity in a mixture of substrate. For photocatalysis the dye degradation efficiency is considered as relative activity for comparison. Catalytic activity in individual substrate was considered as 100%.

Conclusion

In summary we have demonstrated a simple strategy to fabricate dual catalytic microcapsules by immobilizing mpg-C_3N_4-enzyme nanoconjugates at oil-water interface. MCs consisted of two catalyst components perform individual catalytic cycle separately in their respective substrate. Interestingly, these MCs are able to execute photocatalysis and biocatalysis simultaneously in a mixture of substrate without much compromising their activity. This approach will open up the avenue for biomedical waste treatment

where mixture of pollutants needs to be degraded in minimum number of cycle.

Acknowledgements

DP thanks Prof. U. C. Banerjee and Dr. B. P. Dwivedee (National Institute of Pharmaceutical Education and Research, SAS Nagar, 160062, Punjab, India) for helpful discussions. DP also thanks Dr. S. Vaidya (INST, Mohali, India) for important suggestions. DP acknowledges the financial support by SERB-DST (ECR/2017/000442). KG is thankful to get financial support by Nanomission (SR-/NM/NS-91/2016), Department of Science and Technology, Govt. of India.

Notes and references

1. J. J. Zhang, D. L. Mauzerall, T. Zhu, S. Liang, M. Ezzati and J. Remais, *Lancet*, 2010, **375**, 1110.
2. D. Setyorini, T. Prihatini, U. Kurnia and J. I. J. No, *Pollution of soil by agricultural and industrial waste*, Food and Fertilizer Technology Center, 2002.
3. V. Geissen, H. Mol, E. Klumpp, G. Umlauf, M. Nadal, M. van der Ploeg, S. E. van de Zee and C. J. Ritsema, *International Soil and Water Conservation Research*, 2015, **3**, 57-65.
4. P. Verlicchi, A. Galletti, M. Petrovic and D. Barceló, *J. Hydrol.*, 2010, **389**, 416-428.
5. A. Kot-Wasik, D. Dąbrowska and J. Namieśnik, *J. Photochem. Photobiol. A: Chemistry*, 2004, **168**, 109-115.
6. R. M. Baena-Nogueras, E. González-Mazo and P. A. Lara-Martín, *Sci. Total Environ.*, 2017, **590**, 643-654.
7. M. M. Mahlambi, C. J. Ngila and B. B. Mamba, *J. Nanomater.*, 2015, **2015**, 5.
8. I. S. Yunus, Harwin, A. Kurniawan, D. Adityawarman and A. Indarto, *Environmental Technology Reviews*, 2012, **1**, 136-148.
9. Q. Zheng, H. Shen and D. Shuai, *Environ. Sci.: Water Res. Technol.*, 2017, **3**, 982-1001.
10. M. Rao, R. Scelza, R. Scotti and L. Gianfreda, *J. Soil Sci. Plant Nut.*, 2010, **10**, 333-353.
11. I. M. Banat, P. Nigam, D. Singh and R. Marchant, *Bioresour. Technol.*, 1996, **58**, 217-227.
12. A. Marco, S. Esplugas and G. Saum, *Water Sci. Technol.*, 1997, **35**, 321-327.
13. G. Li, S. Park, D.-W. Kang, R. Krajmalnik-Brown and B. E. Rittmann, *Environ. Sci. Technol.*, 2011, **45**, 8359-8367.
14. I. Oller, S. Malato and J. Sánchez-Pérez, *Science of the total environment*, 2011, **409**, 4141-4166.
15. P. Van Aken, N. Lambert, R. Van den Broeck, J. Degrève and R. Dewil, *Environ. Sci.: Water Res. Technol.*, 2019, **5**, 444-481.
16. P. Zapata, J. Faria, M. Ruiz, R. E Jentoft and D. Resasco, *Hydrophobic Zeolites for Biofuel Upgrading Reactions at the Liquid-Liquid Interface in Water/Oil Emulsions*, 2012.
17. D. Patra, A. Sanyal and V. M. Rotello, *Chem. Asian J.*, 2010, **5**, 2442-2453.
18. X.-R. Wei, J. Liu, Y. Yang and L. Deng, *RSC Adv.*, 2014, **4**, 35744-35749.
19. J. Potier, S. Menuel, M.-H. Chambrier, L. Burylo, J.-F. Blach, P. Woisel, E. Monflier and F. Hapiot, *ACS Catal.*, 2013, **3**, 1618-1621.
20. J. Faria, M. Pilar Ruiz and D. E. Resasco, *ACS Catal.*, 2015, **5**, 4761-4771.
21. L. Leclercq, A. Mouret, A. Proust, V. Schmitt, P. Bauduin, j.-m. Aubry and V. Nardello-Rataj, *Pickering Emulsion Stabilized by Catalytic Polyoxometalate Nanoparticles: A New Effective Medium for Oxidation Reactions*, 2012.
22. S. Crossley, J. Faria, M. Shen and D. E. Resasco, *Science*, 2010, **327**, 68-72.
23. C. Wu, S. Bai, M. B. Ansorge-Schumacher and D. Wang, *Adv. Mater.*, 2011, **23**, 5694-5699.
24. H. Jiang, Y. Li, L. Hong and T. Ngai, *Chem. Asian J.*, 2018, **13**, 3533-3539.
25. R. Jain and C. S. Gopinath, *ACS Appl. Mater. Interfaces*, 2018, **10**, 41268-41278.
26. Z. Wang, M. C. M. van Oers, F. P. J. T. Rutjes and J. C. M. van Hest, *Angew. Chem. Int. Ed.*, 2012, **51**, 10746-10750.
27. H. Wanyika, E. Gatebe, P. Kioni, Z. Tang and Y. Gao, *Afr. J. Pharm. Pharmaco.*, 2011, **5**, 2402-2410.
28. J. Xu and M. Antonietti, *J. Am. Chem. Soc.*, 2017, **139**, 6026-6029.
29. B. Samanta, X.-C. Yang, Y. Ofir, M.-H. Park, D. Patra, S. S. Agasti, O. R. Miranda, Z.-H. Mo and V. M. Rotello, *Angew. Chem. Int. Ed.*, 2009, **48**, 5341-5344.
30. M. M. Bradford, *Anal. Biochem.*, 1976, **72**, 248-254.
31. N. Gupta, P. Rathi and R. Gupta, *Anal. Biochem.*, 2002, **311**, 98-99.
32. Y. Jeong, B. Duncan, M.-H. Park, C. Kim and V. M. Rotello, *Chem. Commun.*, 2011, **47**, 12077-12079.
33. H. Sun, Y. Cao, L. Feng and Y. Chen, *Sci. Rep.*, 2016, **6**, 22808.
34. A. Pandey, G. Naresh and T. K. Mandal, *Sol. Energy Mater. Sol. Cells*, 2017, **161**, 197-205.

Journal Name ARTICLE

View Article Online
DOI: 10.1039/C9NJ05322K

TOC: